Journal of Materials Chemistry B

Accepted Manuscript

ROYAL SOCIETY OF CHEMISTRY

www.rsc.org/materialsB

Journal of
Materials Chemistry B

PAPER

Tetrahydro-β-carboline-3-carboxyl-thymopentin: A nano-conjugate for releasing pharmacophores to treat tumor and complications

Xi Hu,[a] Ming Zhao,[a,b*] Yuji Wang,[a] Yaonan Wang,[a] Shurui Zhao,[a] Jianhui Wu,[a] Xiangmin Li,[c] and Shiqi Peng[a,*]

To improve the therapeutic efficacy of cancer patients a novel conjugate of thymopentin (TP5) and (1S,3S)-1-methyl-tetrahydro-β-carboline-3-carboxylic acid (MTC) was presented. In water and mouse plasma MTCTP5 forms the nanoparticles of 14-139 nm in diameter, the suitable size for delivery in blood circulation. In mouse plasma MTCTP5 releases MTC, while in presence of trypsin MTCTP5 releases MTC and TP5. On mouse and rat models MTCTP5 dose dependently slows tumor growth, inhibits inflammatory response and blocks thrombosis. The anti-tumor activity as well as the anti-inflammation activity and anti-thrombotic activity of MTCTP5 are 100 folds and 10 folds higher than those of MTC, respectively, which is attributed to it down-regulates plasma levels of TNF-α and IL-8 of the treated animals. The immunologic enhancing activities *in vitro* and *in vivo* of MTCTP5 are similar to that of TP5, which is attributed to MTCTP5 up-regulates the plasma levels of IL-2 and CD4 as well as down-regulates the plasma level of CD8 of the treated animals. The plasma alanine transaminase, aspartate transaminase and creatinine assays indicate MTCTP5 therapy does not injure the liver and the kidney of the animals. The survival time of MTCTP5 treated mice is significantly longer than that of TP5 treated mice.

Received 00th January 20xx
Accepted 00th January 20xx

DOI:10.1039/x0xx00000x

www.rsc.org/MaterialsB

Introduction

Thymopentin (TP5, RKDVY), the Arg32-Tyr36 fragment of the thymus hormone thymopoietin, is well known as immunomodulator, has important role in T-lymphocyte maturation and differentiation, and is used in the clinic to treat some immunodeficiencies, malignancies and infections[1-3]. However, TP5 has very short half-life *in vivo* and can be administered either via intramuscular injection or via intravenous infusion.[4] Additionally TP5 is successfully used as a pharmacophore or an activity enhancer in the modification of peptides, polymers and formulations for various purposes. Of TP5 modified peptides and polymers TP5-RR-6 peptide is for treating tuberculosis,[5] TP5-thymosin α1 and TP5-iRGD peptides are for treating tumor,[6,7] TP5-poly(butyl cyanoacrylate) is for enhancing immunomodulatory activity,[8] and TP5-PLGA-lectins is for improving oral immune-modulatory activity.[9] Of the formulations TP5 formulated chitosan or bacitracin is a novel intranasal delivery,[10] the co-sprayed dry powders of TP5 with lactose or mannitol are for improving the flow ability,[11] TP5 incorporated copolymer of poly-D-lactide and poly(ethylene glycol) is for slowing release rate,[12] the aerosol is for improving systemic action of TP5,[13] and the mixed polymer matrix of polylactide and poly(lactic-co-glycolic) of TP5 is for preparing biodegradable microspheres.[14]

β-Carbolines have diverse pharmacological functions, such as inhibiting platelet activation,[15] improving object recognition memory,[16] stimulating insulin secretion,[17] interacting with DNA,[18,19] and blocking topoisomerases.[20] Besides, β-carbolines are the pharmacophores of a series of bioactive agents, such as trypanocidal agents,[21] anti-malarial agents,[22,23] neuron-protective and neuron-differentiating agents,[24] antiviral agent,[25] anti-leishmanial agent,[26] as well as antitumor agents,[27-30] anti-inflammatory agents,[31] and anti-thrombotic agents in particular.[32,33]

It is well known that chronic inflammation can increase cancer susceptibility, while anti-inflammatory drugs may retard the development of cancers.[34,35] Long-term and low-dose administration of aspirin is associated with lower cancer mortality, suggesting anti-thrombotic therapy benefits the outcome of cancer patients.[36] Thrombotic microangiopathy (TMA) is now recognized as a late complication of cancers.[37]

[a]Beijing area major laboratory of peptide and small molecular drugs; Engineering Research Center of Endogenous Prophylactic of Ministry of Education of China; Beijing Laboratory of Biomedical Materials; College of Pharmaceutical Sciences, Capital Medical University, Beijing 100069, P.R. China
[b]Faculty of Biomedical Science and Environmental Biology, Kaohsiung Medical University, Kaohsiung, Taiwan
[c]Jiangxi-OAI Joint Research Institute, Nanchang University, Nanchang 330047, PR China
*To whom correspondence should be addressed. SP: College of Pharmaceutical Sciences, Capital University of Medical Sciences, Beijing 100069, P.R. China. Tel: 86-10-8391-1528, Fax: 86-10-8391-1528, E-mail: sqpeng@bjmu.edu.cn; MZ: Tel.: +86-10-8280-2482, fax: +86-10-8280-2482, E-mail: mingzhao@bjmu.edu.cn

Several clinical studies indicate that TMA can develop directly from certain malignancies, but more often results from anticancer therapy.[38] These findings emphasize the potential utility of a pharmacophore capable of simultaneously inhibiting cancer, thrombosis and inflammation. Our broad screening identified that (1S,3S)-1-methyltetrahydro-β-carboline-3-carboxylic acid (MTC) is such a pharmacophore.[32,33] However, the antitumor, anti-inflammatory and anti-thrombotic activities of MTC need to be enhanced. In this context, the present paper used TP5 as an enhancer of MTC to prepare nano-scale N-[(1S,3S)-1-methyltetrahydro-β-carboline-3-carboxyl]-Arg-Lys-Asp-Val-Tyr (MTCTP5), and to evaluate the bioactivities.

Materials and Methods

General procedures

All L-amino acids were purchased from Sigma-Aldrich Co. (St. Louis, MO, USA). The column chromatography was performed using silica gel (200-300 mesh, Qingdao Haiyang Chemical Co., Qingdao, P. R. China). The purities of MTC, protective TP5 and protective MTCTP5 (>95%) were determined by TLC analysis (Qingdao silica gel plates of GF254). The purity of MTCTP5 (>96%) was determined by HPLC analysis (CHIRALPAK AH-H column, 4.6 × 250 mm, Daicel Chemical IND., LTD).

The spectra of ^{1}H NMR (800 MHz) and ^{13}C NMR (200 MHz) were recorded on Bruker Avance II 800 MHz spectrometer with DMSO-d_6 as the solvent and tetramethylsilane as internal standard. ESI/MS was tested on ZQ 2000 (Waters, US) and solariX FT-ICR mass spectrometer (Bruker Daltonik) consisting of an ESI/MALDI dual ion source and 9.4 T superconductive magnet.

K562, A549, HT-29 and HL-60 carcinoma cell lines were purchased from ATCC. Bovine serum albumin (BSA) was purchased from Sigma. Fetal bovine serum (FBS), basal DMEM medium and 1640 medium were purchased from Gibco.

Male Wistar rats and ICR mice were purchased from the Animal Center of Capital Medical University. The protocol was reviewed and approved by the ethics committee of Capital Medical University. The committee assures that the welfare of the animals was maintained in accordance to the requirements of the Animal Welfare Act and in accordance to the NIH Guide for Care and Use of Laboratory Animals.

All experimental data are presented as the average ± SD. Statistical analyses of all the biological data were carried out by use of ANOVA by SPSS. P-values <0.05 were considered statistically significant.

Synthesis of MTCTP5

MTCTP5 was prepared by use of the synthetic route depicted in scheme 1, the preparations of the related intermediates and the chemical physical data thereof are given in the corresponding procedures.

Preparing (1S,3S)-1-methyl-1,2,3,4-tetrahydro-β-carboline-3-carboxylic acid (1, MTC)

To a solution of 10.0 g (49.0 mmol) of L-Trp, 4 mL of concentrated H_2SO_4 and 400 mL of water 10 mL of aldehyde (40%) was added. The reaction mixture was stirred at room temperature for 6 h, adjusted to pH 7 with concentrated ammonia, and then kept at 0 ºC for 0.5 h. The formed precipitates were collected by filtration to give 8.0 g (70%) of MTC. ESI-MS (m/e): 231 $[M + H]^+$; ^{1}H NMR (300 MHz, DMSO-d_6): δ/ppm = 11.144 (s, 1H), 7.449 (d, J = 7.8 Hz, 1H), 7.349 (d, J = 7.8 Hz, 1H), 7.090 (t, J = 7.2 Hz, 1H), 7.000 (t, J = 7.8 Hz, 1H), 4.536 (d, J = 6.6 Hz, 1H), 3.636 (dd, J = 4.8 Hz, J = 12.0 Hz, 1H), 3.204 (dd, J = 4.8 Hz, J = 12.0 Hz, 1H), 2.792 (m, 1H), 1.630 (d, J = 6.6 Hz, 3H).

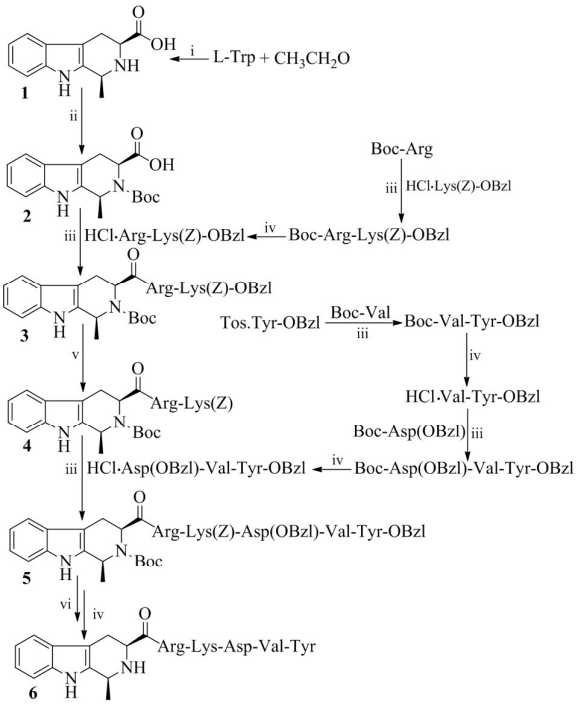

Scheme 1 Synthetic route to MTCTP5. (i) Sulfuric acid; (ii) DMF, Di-tert-butyl dicarbonate (Boc_2O) and triethylamine; (iii) Dicyclohexylcarbodiimide (DCC), N-hydroxybenzotrizole (HOBt), N-methylmorpholine (NMM) and tetrahydrofuran (THF); (iv) Hydro chloride in ethyl acetate (4M); (v) Aqueous NaOH (4M); (vi) H_2, Pd/C and CH_3OH.

Preparing (1S,3S)-1-methyl-2-Boc-1,2,3,4-tetrahydro-β-carboline-3-carboxylic acid (2)

A solution of 8.0 g (34.8 mmol) of MTC and 8.0 g (37.0 mmol) of Boc_2O in 100 mL of DMF was stirred at 0 ºC for 30 min and at room temperature for additional 48 h, evaporated under vacuum, the residue was triturated with ether, the residue was dissolved in 100 mL of water and then was acidified with a

dilute hydrochloric acid to pH 2. The solution was extracted with ethyl acetate (30 mL × 3), the ethyl acetate phase was washed with water (30 mL × 3) and dried with anhydrous sodium sulfate for 12 h. The ethyl acetate phase was filtered and the filtrate was evaporated under vacuum to give 7.6 g (66%) of the title compound as colorless powders. ESI-MS (m/e): 331 $[M + H]^+$.

Preparing Boc-Val-Tyr-OBzl

At 0 ºC a solution of 0.434 g (2.0 mmol) of Boc-Val, 0.270 g (2.0 mmol) of HOBt, 20 mL of anhydrous THF and 0.450 g (2.2 mmol) of DCC was stirred for 30 min, to which a solution of 0.886 g (2.0 mmol) of Tos·Tyr-OBzl in 10 mL of anhydrous THF was added, and adjusted to pH 9 with NMM. The reaction mixture was stirred at room temperature for 8 h and TLC (CH_2Cl_2: CH_3OH, 40:1) indicated complete disappearance of Tos·Tyr-OBzl. The formed precipitates of dicyclohexylurea (DCU) were removed by filtration, the filtrate was evaporated under vacuum and the residue was dissolved in 100 mL of ethyl acetate. The solution was washed successively with 5% aqueous solution of sodium bicarbonate, 5% aqueous solution of citric acid and saturated aqueous solution of sodium chloride. The ethyl acetate phase was dried with anhydrous sodium sulfate for 12 h. After filtration the filtrate was evaporated under vacuum to provide 0.688 g (88%) of the title compound as colorless powders. ESI-MS (m/e): 471 $[M + H]^+$.

Preparing HCl·Val-Tyr-OBzl

At 0 ºC a solution of 0.874 g (1.8mmol) of Boc-Val-Tyr-OBzl in 10 mL solution of hydrogen chloride in ethyl acetate was stirred for 1 h and then evaporated under vacuum. The residue was dissolved in 20 mL of ethyl acetate and the solution was evaporated under vacuum to thoroughly remove the hydrogen chloride and provide 0.701 g (92%) of the title compound as colorless powders for next reaction directly. ESI-MS (m/e): 371 $[M + H]^+$.

Preparing Boc-Asp(OBzl)-Val-Tyr-OBzl

At 0 ºC a solution of 0.578 g (1.8mmol) of Boc-Asp(OBzl), 0.240 g (1.8mmol) of HOBt, 20 mL of anhydrous THF and 0.401 g (2.0mmol) of DCC was stirred for 30 min, to which a solution of 0.758 g (1.8mmol) of HCl·Val-Tyr-OBzl in 10 mL of anhydrous THF was added, and adjusted to pH 9 with NMM. The reaction mixture was stirred at room temperature for 8 h, and TLC (CH_2Cl_2: CH_3OH, 40: 1) indicated complete disappearance of HCl·Val-Tyr-OBzl. The formed DCU precipitates were removed by filtration and the filtrate was evaporated under vacuum, the residue was dissolved in 100 mL of ethyl acetate and the solution was washed successively with 5% aqueous solution of sodium bicarbonate, 5% aqueous solution of citric acid and saturated aqueous solution of sodium chloride. The ethyl acetate phase was dried with anhydrous sodium sulfate for 12 h. After filtration the filtrate was evaporated under vacuum to provide 1.004 g (82%) of the title compound as colorless powders. ESI-MS (m/e): 676 $[M + H]^+$.

Preparing HCl·Asp(OBzl)-Val-Tyr-OBzl

Using the procedure preparing HCl·Val-Tyr-OBzl from 1.004 g (1.5mmol) of Boc-Asp(OBzl)-Val-Tyr-OBzl 0.687 g (91%) of the title compound was obtained as colorless powders for the next reaction directly. ESI-MS (m/e): 576 $[M + H]^+$.

Preparing Boc-Arg-Lys(Z)-OBzl

At 0 ºC a solution of 0.552 g (3.0 mmol) of Boc-Arg, 0.405 g (3.0 mmol) of HOBt, 0.675 g (3.6 mmol) of DCC and 20 mL of anhydrous THF was stirred for 30 min, to which a solution of 1.629 g (3.0 mmol) of Tos·Lys(Z)-OBzl in 10 mL of anhydrous THF was added, and adjusted to pH 9 with NMM. The reaction mixture was stirred at room temperature for 8 h and TLC (CH_2Cl_2: CH_3OH, 10:1) indicated complete disappearance of Tos·Lys(Z)-OBzl. The formed DCU precipitates were removed by filtration and the filtrate was evaporated under vacuum. The residue was dissolved in 100 mL of ethyl acetate. The solution was washed successively with 5% aqueous solution of sodium bicarbonate, 5% aqueous solution of citric acid and saturated aqueous solution of sodium chloride. The ethyl acetate phase was dried with anhydrous sodium sulfate for 12 h. After filtration the filtrate was evaporated under vacuum to provide 1.428 g (74%) of title compound as colorless powders. ESI^+-MS (m/e): 627 $[M + H]^+$.

Preparing HCl·Arg-Lys(Z)-OBzl

Using the procedure preparing HCl·Val-Tyr-OBzl from 1.290 g (2.0 mmol) of Boc-Arg-Lys(Z)-OBzl 1.021 g (92%) of the title compound was obtained as colorless powders for next reaction directly. ESI-MS (m/e): 527 $[M + H]^+$.

Preparing (1S,3S)-1-methyl-2-Boc-1,2,3,4-tetrahydro-β-carboline-3-carboxyl-Arg-Lys(Z)-OBzl (3)

At 0 ºC a solution of 0.506 g (2.2 mmol) of (1S,3S)-1-methyl-2-Boc-1,2,3,4-tetrahydro-β-carboline-3-carboxylic acid, 0.270 g (2.0 mmol) of HOBt, 0.490 g (2.4 mmol) of DCC and 20 mL of anhydrous THF was stirred for 30 min, to which a solution of 1.116 g (2.0 mmol) of HCl·Arg-Lys(Z)-OBzl in 10 mL of anhydrous THF was added, and adjusted to pH 9 with NMM. The reaction mixture was stirred at room temperature for 8 h and TLC (CH_2Cl_2: CH_3OH, 20:1) indicated complete disappearance of HCl·Arg-Lys(Z)-OBzl. The formed DCU precipitates were removed by filtration, the filtrate was evaporated under vacuum and the residue was dissolved in 100 mL of dichloromethane. The solution was washed successively with 5% aqueous solution of sodium bicarbonate, 5% aqueous solution of citric acid and saturated aqueous solution of sodium chloride. The dichloromethane phase was dried with anhydrous sodium sulfate for 12 h. After filtration the filtrate was evaporated under vacuum to provide 1.178 g (70%) of the title compound as colorless powders for next reaction directly. ESI-MS (m/e): 839 $[M + H]^+$.

Preparing (1S,3S)-1-methyl-2-Boc-1,2,3,4-tetrahydro-β-carboline-3-carboxyl-Arg-Lys(Z) (4)

At 0 ºC a solution of 1.178 g (1.4mmol) of (1S,3S)-1-methyl-2-Boc-1,2,3,4-tetrahydro-β-carboline-3-carboxyl-Arg-Lys(Z)-OBzl, 10 mL of methanol and 2 mL of aqueous NaOH (2 M) was stirred for 60 min, adjusted to pH 2 with hydrochloric acid (2 M) and evaporated under vacuum. The residue was dissolved in 100 mL of ethyl acetate and the solution was dried with anhydrous sodium sulfate for 12 h. After filtration the filtrate was evaporated under vacuum to provide 1.046 g (99%) of the title compound as colorless powders for next reaction directly. ESI-MS (m/e): 749 $[M + H]^+$.

Preparing (1S,3S)-1-methyl-2-Boc-1,2,3,4-tetrahydro-β-carboline-3-carboxyl-Arg-Lys(Z)-Asp(OBzl)-Val-Tyr-OBzl (5)

At 0 ºC a solution of 0.773 g (1.0 mmol) of (1S,3S)-1-methyl-2-Boc-1,2,3,4-tetrahydro-β-carboline-3-carboxyl-Arg-Lys(Z), 0.135g (1.0 mmol) of HOBt, 0.244 g (1.2 mmol) of DCC and 20 mL of anhydrous THF was stirred for 30 min, to which a solution of 0.610 g (1.0 mmol) of HCl·Asp(OBzl)-Val-Tyr-OBzl in 10 mL of anhydrous THF was added, and adjusted to pH 8 with NMM. The reaction mixture was stirred at room temperature for 48 h and TLC (CH_2Cl_2: CH_3OH, 10:1) indicated complete disappearance of HCl·Asp(OBzl)-Val-Tyr-OBzl. The formed DCU precipitates were removed by filtration, the filtrate was evaporated under vacuum and the residue was dissolved in 100 mL of dichloromethane. The solution was washed successively with 5% aqueous solution of sodium bicarbonate, 5% aqueous solution of citric acid and saturated aqueous solution of sodium chloride. The dichloromethane phase was dried with anhydrous sodium sulfate for 12 h. After filtration the filtrate was evaporated under vacuum to provide 0.824 g (68%) of the title compound as colorless powders. ESI-MS(*m/e*): 1307 $[M + H]^+$; ^{1}H-NMR (300 MHz, DMSO-d_6): δ/ppm = 10.910 (s, 1H), 9.292 (s, 1H), 8.455 (m, 2H), 8.166 (m, 1H), 7.531 (m, 2H), 7.312 (m, 15H), 7.223 (m, 4H) , 6.976 (d, J = 2.7 Hz, 2H), 6.652 (d, J = 2.7 Hz, 2H), 5.001 (m, 7H), 4.683 (m, 1H), 4.438 (m, 1H), 4.306 (m, 3H), 3.233 (m, 1H), 3.168 (m, 2H), 2.949-2.785 (m, 6H), 2.665 (m, 1H), 1.929 (m, 1H), 1.540-1.247 (m, 21H), 0.729 (dd, J = 7.5 Hz, J = 15.0 Hz, 6H).

Preparing (1S,3S)-1-methyl-1,2,3,4-tetrahydro-β-carboline-3-carboxyl-Arg-Lys-Asp-Val-Tyr (MTCTP5, 6)

To a suspension of 0.100 g (0.077 mmol) of (1S,3S)-1-methyl-2-Boc-1,2,3,4-tetrahydro-β-carboline-3-carboxyl-Arg-Lys(Z)-Val-Tyr-OBzl, 20 mL of methanol, 0.2 mL of formic acid and 20 mg of Pd/C (10%) hydrogen gas was bubbled for 20 h and TLC indicates complete disappear of (1S,3S)-1-methyl-2-Boc-tetrahydro-β-carboline-3-carboxyl-Arg-Lys(Z)-Val-Tyr-OBzl. The reaction mixture was filtered and the filtrate was evaporated under vacuum. The residue was treated with 10 mL of ethyl acetate containing hydrogen chloride (4 M) to remove Boc. After removal of hydrogen chloride 0.056 g (63%) of the title compound was obtained as colorless powders. Mp 123 - 124 ºC; $[\alpha]_D^{25}$ = -89.0 (c 0.10, CH_3OH); FT-MS (*m/e*): 892.47541 $[M + H]^+$; HPLC purity (CH_3OH:H_2O= 95%:5%, C_{18}, 1.0 mL/min): 96%.^{1}H-NMR (800 MHz, DMSO-d_6): δ/ppm = 11.287 (s, 1H), 9.246 (s, 1H), 8.946 (s, 1H), 8.532 (s, 1H), 8.257 (s, 1H), 8.194 (d, J = 8.0 Hz, 1H), 8.005 (s, 3H), 7.485 (d, J = 8.0 Hz, 1H), 7.472 (m, 1H), 7.432 (d, J = 8.0 Hz, 1H), 7.383 (m, 1H), 7.130 (t, J = 8.0 Hz, 1H), 7.040 (t, J = 8.0 Hz, 1H), 6.974 (t, J = 8.0 Hz, 2H), 6.657 (d, J = 8.0 Hz, 2H), 4.722 (m, 1H), 4.567 (m, 1H), 4.433 (m, 1H), 4.315 (m, 2H), 4.225 (m, 1H), 3.122 (m, 3H), 2.896 (m, 2H), 2.898 (m, 2H), 2.785 (m, 1H), 2.753 (m, 2H), 2.672 (m, 1H), 2.562 (m, 1H), 1.984 (m, 1H), 1.859 (m, 1H), 1.694 (d, J = 6.4 Hz, 3H), 1.645-1.241 (m, 8H), 0.799 (dd, J = 7.2 Hz, J = 24.0 Hz, 6H); ^{13}C-NMR (200 MHz, DMSO-d_6): δ/ppm = 173.30, 171.95, 171.26, 171.06, 170.64, 157.53, 156.42, 136.85, 130.43, 128.55, 127.85, 126.20, 125.97, 125.95, 122.16, 119.70, 118.40, 115.48, 111.90, 105.29, 57.47, 56.37, 54.35, 52.99, 52.73, 50.09, 49.85, 49.06, 36.36, 31.53, 27.00, 25.43, 23.94, 22.54, 19.60, 18.04, 16.91; IR (KBr): 3167.12, 3059.20, 2962.66, 2931.80, 2873.94, 1720.50, 1654.92, 1543.05, 1516.05, 1450.47, 1396.46, 1319.31, 1226.73.

Preparing Boc-Arg-Lys(Z)-Asp(OBzl)-Val-Tyr-OBzl

At 0 ºC a solution of 0.627 g (1.0 mmol) of Boc-Arg-Lys(Z)-OBzl, 10 mL of methanol and 2 mL of aqueous NaOH (2M) was stirred for 60 min, adjusted to pH 7 with hydrochloric acid (2 M), and evaporated under vacuum. The residue was dissolved in 100 mL of THF, mixed with 0.135 g (1.0 mmol) of HOBt and 0.244 g (1.2 mmol) of DCC, stirred at 0 ºC for 30 min, to which a solution of 0.550 g (0.9 mmol) of HCl·Asp(OBzl)-Val-Tyr-OBzl in 10 mL of anhydrous THF was added, and adjusted to pH 8 with NMM. The reaction mixture was stirred at room temperature for 48 h and TLC (CH_2Cl_2: CH_3OH, 10:1) indicated the disappearance of HCl·Asp(OBzl)-Val-Tyr-OBzl. The formed DCU precipitates were removed by filtration, the filtrate was evaporated under vacuum, the residue was dissolved in 100 mL of CH_2Cl_2, and the solution was successively washed with 5% aqueous solution of sodium bicarbonate, 5% aqueous solution of citric acid and saturated aqueous solution of sodium chloride. The CH_2Cl_2 phase was dried with anhydrous sodium sulfate for 12 h. After filtration the filtrate was evaporated under vacuum to provide 0.564 g (57%) of the title compound as colorless powders. ESI-MS(*m/e*): 1095 $[M + H]^+$; ^{1}H-NMR (300 MHz, DMSO-d_6): δ/ppm = 8.441 (m, 2H), 7.803 (m, 2H), 7.597-7.434 (m, 4H), 7.321-7.223 (m, 15H) , 7.140(d, J = 8.4 Hz, 2H), 6.938 (d, J = 8.4 Hz, 2H), 5.031 (m, 6H), 4.666 (m, 1H), 4.502 (m, 1H), 4.260 (m, 2H), 3.918 (m, 1H), 3.165 (m, 2H), 3.012-2.778 (m, 6H), 1.923 (m, 1H), 1.722-1.485 (m, 6H), 1.369-1.238(m, 13H), 0.743(m, 6H).

Preparing Arg-Lys-Asp-Val-Tyr (TP5)

To a suspension of 0.100 g (0.091 mmol) of Boc-Arg-Lys(Z)-Val-Tyr-OBzl, 20 mL of methanol, 0.2 mL of formic acid and 20 mg of Pd/C (10%) hydrogen gas was bubbled for

20 h and TLC indicates complete disappear of Boc-Arg-Lys(Z)-Asp(OBzl)-Val-Tyr-OBzl. The reaction mixture was filtered, the filtrate was evaporated under vacuum and the residue was treated with 10 mL of ethyl acetate containing hydrogen chloride (4 M) to remove Boc. After removal of hydrogen chloride 0.036 g (58%) of the title compound was obtained as colorless powders. ESI-MS(*m/e*): 680 $[M + H]^+$; ^{1}H-NMR (300 MHz, D_2O): δ/ppm = 7.039 (d, J = 8.4 Hz, 2H), 6.628 (d, J = 8.4 Hz, 2H), 4.606-4.525 (m, 2H), 4.323 (m, 1H), 3.984-3.871 (m, 2H), 3.151-3.040 (m, 3H), 2.922-2.819 (m, 3H), 2.802-2.603 (m, 2H), 1.925-1.502 (m, 9H), 1.419-1.312 (m, 2H), 0.738 (m, 6H).

Trypsin promoted release of MTCTP5

To a solution of MTCTP5 (1 μM) in ultrapure water 200μL of trypsin (800 UI) was added, at 37 °C incubated for 10, 20, 30, and 60 min, and 10 μL of the supernatant was used to carry out ESI-MS experiments using positive and negative MALDI ion modes.

Mouse plasma stability of MTCTP5

Mouse blood was collected in 1 mg/mL aqueous solution of heparin sodium (1:9, v/v) and immediately centrifuged at 3000 rpm for 15 min to collect the plasma. To 200 μL of plasma 200 μL solution of MTCTP5 (2 μM) in ultrapure water was added and incubated at 37 °C for 10, 20, 30, 60 and 90 min. To the plasma 800 μL of methanol was added and the sample was centrifuged at 3000 rpm for 10 min, and then 10 μL of the supernatant was used to carry out the ESI-MS experiment.

Measuring FT-MS spectra of MTCTP5

The positive MALDI FT-MS spectrum of aqueous solution of MTCTP5 (10^{-6} nM) was measured on a solariX FT-ICR mass spectrometer (Bruker Daltonics, Billerica, MA, USA) having an ESI/MALDI dual ion source and a 9.4 T superconductive magnet. The ion source was a Smart-beam-II laser (wavelength, 355 nm; focus setting, 'medium'; repetition rate, 1000 Hz). The QCID spectrum was set to 2000 m/z, and the isolation window was 5 m/z. Data were collected with solariX-control software. Spectral data were processed with data analysis software (Bruker Daltonics).

Measuring NOESY 2D NMR spectra of MTCTP5

One-dimensional ^{1}H NMR spectra of 12 mg of MTCTP5 in 0.5 mL of deuteron dimethyl sulfoxide (DMSO-d_6) were measured on a Bruker 800MHz spectrometer. The probe temperature was regulated to 298 K. Using a simple pulse-acquire sequence zg30 the spectra were recorded. To ensure full relaxation of ^{1}H resonance typical acquisition parameters consisted of 64 K points covering a sweep width of 16447 Hz, a pulse width (pw90) of 8.63 μs and a total repetition time of 24 s were used. Before FT the digital zero filling to 64 K and a 0.3 Hz exponential function were applied to the FID. The resonance at 2.5 ppm presented CD_2HSOCD_2H (the impurity in the residual solvents) and tetramethylsilane (TMS) was used as internal reference. Standard absorptive 2D ^{1}H-^{1}H COSY was measured with the same spectrometer. Each spectrum consisted of a matrix of 2 K (F2) by 0.5 K (F1) covering a sweep width of 9615.4 Hz. Before FT the matrix was zero filled to 1 K by 1 K and the standard sinebell apodization functions were applied in both dimensions. 2D NOESY tests were carried out in the phase-sensitive mode by using the same spectrometer. Spectra were obtained using spin-lock mixing periods of 200 ms.

Measuring TEM image of MTCTP5

Shape and size of the nanospecies of MTCTP5 in water were measured with transmission electron microscopy (TEM, JSM-6360 LV, JEOL, Tokyo, Japan). In brief, an aqueous solution of MTCTP5 (pH 6.7, 10^{-7} nM) was dripped onto a formvar-coated copper grid. The grid was allowed to dry thoroughly in air and then was heated at 35 °C for 14 days. The copper grids were viewed under TEM. The shape and size distribution of the nanospecies were determined by counting >100 species in randomly selected regions on the copper grid. Each determination was carried out with triplicate grids and at 80 kV (the electron beam accelerating voltage). Images were recorded on an imaging plate (Gatan Bioscan Camera Model 1792, Pleasanton, CA, USA) with 20 eV energy windows at 6000 - 400,000× and were digitally enlarged.

Measuring SEM images of MTCTP5

The shape and size of the nanospecies of MTCTP5 in solid state were measured by scanning electron microscopy (SEM, JEM-1230, JEOL, Tokyo, Japan) at 50 kV. In brief, the lyophilized powders from 10^{-7} nM solution of MTCTP5 in ultrapure water were attached to a copper plate with double-sided tape (Euromedex, Strasbourg, France). The specimens were coated with 20 nm gold-palladium using a Joel JFC-1600 Auto Fine Coater. The coater was operated at 15 kV, 30 mA, and 200 mTorr (argon) for 60 s. The shape and size distribution of the nanospecies were measured by examining >100 species in randomly selected regions on the SEM alloy. Each measurement was performed with triplicate grids. Images were recorded on an imaging plate (Gatan Bioscan Camera Model 1792) with 20 eV energy windows at 100 - 10,000 ×, and were digitally enlarged.

Measuring AFM images of MTCTP5

Atomic force microscopy (AFM) experiments were performed using the contact mode on a Nanoscope 3D AFM (Veeco Metrology, Santa Barbara, CA, USA) in ambient conditions. AFM images of mouse plasma alone or MTCTP5 in mouse plasma (10^{-7} nM) were recorded with a standard procedure.

Measuring particle size of MTCTP5

The particle size of MTCTP5 in ultrapure water was measured on a Particle Size Analyzer (Zeta Plus S/N 21394,

Brookhaven Instruments Corporation) with dynamic light scattering (DLS) model. The concentration of the solution of MTCTP5 in ultrapure water was 10^{-7} nM and the testing temperature was 25 °C. The Size measurement was repeated for 3 runs per sample every day, and totally tested for 7 consecutive days.

Measuring zeta potential of the nanospecies of MTCTP5

The surface zeta potential of the nanospecies of MTCTP5 in ultrapure water or in mouse plasma was measured on a ZetaPlus Potential Analyzer (ZetaPlus S/N 21394, Brookhaven Instruments Corporation) with BIC Zeta Potential Analyzer. The concentration of the solution of MTCTP5 in ultrapure water or in mouse plasma was 10^{-7} nM and the testing temperature was 25 °C. The zeta potential measurement was repeated for 3 runs per sample, and the data were calculated automatically using the software from the electrophoretic mobility based on Smoluchowski's formula.

Energy-minimization conformations of MTCTP5

MTCTP5 was sketched in ChemDraw 10.0, converted to 3D conformation in Chem3D 10.0 and then energy minimized in Discovery Studio 3.5 with MMFF force field. The energy-minimized conformation was utilized as the starting one for conformation generation. The energy-minimized conformations were sampled in the whole conformational space via systematic search and BEST methods in Discovery Studio 4.0. Both of the systematic search and BEST methods were practiced with SMART minimizer with CHARMm force field. The energy threshold was set to 20 kcal/mol at 300 K. The maximum minimization steps and RMS gradient were set to 200 Å and 0.1 Å, respectively. The maximum generated conformations were set to 255 with a RMSD cut off 0.2 Å.

Molecular docking of MTCTP5 towards the active site of bovine trypsin

The 3D structure of MTCTP5 was built using a 3D-sketcher module and energy minimized in Discovery Studio 4.0 with SMART minimizer using the CHARMm force field. The crystal structure of bovine trypsin (PDB ID: 4MTB) was from the Protein Data Bank, and the binding sphere (9.0Å) of (2R)-2-amino-N-{(2S)-1-[(4-carbamimi-doylbenzyl)amino]-1-oxopro-pan-2-yl}-4-(4-hydroxyphenyl)-butanamide domain was defined. The water molecules were removed, and hydrogen atoms were added under the CHARMm force field. Docking calculations were performed with LibDock module implemented in Accelrys Discovery studio 4.0, which is a high-through put docking algorithm that positions catalyst generated ligand conformations in the protein active site based on polar and apolar interaction sites (hotspots). The results could be displayed by analyzing and scoring docked ligand poses. To find a top rank pose and measure the goodness of a docking study, LibDock Score was used as the criteria. The binding site "hotspots" were set to 100. The conformation generation of the ligands was using BEST method. The energy threshold was set to 20 kcal/mol, the maximum minimization steps were set to 1000, the minimization RMS gradient was set to 0.001 Å, and the maximum generated conformations were set to 255 with a RMSD cut off 1.0 Å.

***In vivo* xylene-induced ear edema assay**

Male ICR mice were 10 weeks old at the beginning of experiment, randomly divided into 6 groups (12 per group) and intraperitoneally administered with MTCTP5 (2, 0.2 and 0.02 μmol/kg) or MTC (2 μmol/kg) or aspirin (1100 μmol/kg) or NS (10 mL/kg). Thirty min after the administration 0.03 mL of xylene was applied to the anterior and posterior surfaces of right ears of the mice, and left ears without xylene application were used as the controls. Two hours after xylene application the mice were anesthetized with ether and sacrificed for removal of both ears. Using a cork borer of 7 mm in diameter the ears were punched to take circular pieces for weighing. Ear edema was represented with the weight difference between the circular pieces of right and left ears.

***In vivo* anti-thrombotic assay**

Male Wistar rats (250-300 g) were randomly divided into 6 groups (12 per group), and MTCTP5 (2, 0.2 and 0.02 μmol/kg) or MTC (2 μmol/kg) or aspirin (167 μmol/kg) or NS (10 mL/kg) was intraperitoneally administered. Thirty min after the administration the rats were anesthetized with intraperitoneally pentobarbital sodium (80.0 mg/kg), right carotid artery and left jugular vein were separated. A weighed 6 cm thread was inserted into the middle of a polyethylene tube. The polyethylene tube was filled with NS solution of heparin sodium (50 IU/mL) and one end was inserted into left jugular vein. From other end of the polyethylene tube heparin sodium was injected as anticoagulant and this end was inserted into right carotid artery. Blood was allowed to flow from right carotid artery to left jugular vein through the polyethylene tube for 15 min. The thread was removed to obtain the weight of the wet thrombus.

***In vivo* anti-tumor assay**

Male ICR mice were 10-12 weeks old at the beginning of experiments. S180 cells for initiation of subcutaneous tumors were obtained in ascitic form of the mouse tumors, which were serially transplanted once per week. Subcutaneous tumors were implanted by injecting 0.2 mL of NS containing 1.8×10^{7} viable tumor cells under the skin on right oxter. Twenty four hours after implantation the tumor bearing mice were randomized into 6 experimental groups (12 per group). All mice were given a daily intraperitoneal injection of doxorubicin (2 μmol/kg/day in NS) or MTC (2 μmol/kg/day in NS) or NS (10 mL/kg/day) or MTCTP5 (0.002, 0.02, 0.2 and 2 μmol/kg/day in NS) for 12 consecutive days. Twenty four h after the last administration, all mice were sacrificed by ether anesthesia and the tumors were dissected and weighed.

***In vivo* carbon clearance assay**

In vivo carbon clearance assay was performed with a standard procedure. In brief, ICR mice were divided into 3 groups of 10 animals each and given a daily intraperitoneal injection of MTCTP5 (2 μmol/kg/day in NS) or TP5 (positive control, 2 μmol/kg/day in NS) or NS (blank control, 10 mL/kg/day) or for 7 consecutive days. On 8th day the mice were intraperitoneally injected a suspension of 0.1 mL of indian ink and NS solution of gelatine (1%, w/v). One and ten min after the administration the blood was sampled, mixed with aqueous Na_2CO_3 (0.1%, 4 mL) and the absorbance was measured at 660 nm to calculate carbon clearance based on $m_{body}/(m_{liver}+ m_{spleen}) \times [(LogOD1-LogOD2)/9]^{1/3}$,wherein OD1 refers the absorbance at 10 min and OD2 refers the absorbance at 1 min, m_{body}, m_{liver} and m_{spleen} refer the bodyweight, liver weight and spleen weight of the tested mice, respectively.

***In vivo* IL-2, CD4 and CD8 assays**

0.9 mL blood of the mice receiving carbon clearance assay was collected into a syringe containing 0.1 mL of 3.8% sodium citrate and immediately centrifuged at 3000 rpm for 10 min. The separated plasma was used to measure plasma levels of IL-2, CD4 and CD8 by ELISA according to the manufacturer's protocols. In brief 100 μL of plasma or standard solution was added into the wells of anti-body coated 96 microtiter plates, incubated at 37 ºC for 90 min, and washed with 100 μL of wash buffer for 5 times; 100 μL of biotinylated antibody was added, incubated at 37 ºC for 60 min, and washed with 100 μL of wash buffer for 5 times; 100 μL HRP-conjugate reagent was added, incubated at 37 ºC for 30 min, and washed with 100 μL of wash buffer for 5 times; 50 μL of chromogen solution A and 50 μL of chromogen solution B was added, and incubated at 37 ºC for 15 min; 100 μL of stop solution was added, and the absorbance of the yellow solutions were recorded at 450 nm.

***In vitro* spleen lymphocyte proliferation assay**

The effects of MTCTP5 on Babl/c spleen lymphocyte proliferation were measured using MTT assay. The spleen lymphocytes were prepared according to a standard procedure. In brief in sterile conditions after rapid collection spleens were placed in cold RPMI-1640 containing 10% FCS supplemented with antibiotics (100 UI/mL penicillin and 100 mg/mL streptomycin). Cells were teased apart and gently passed through a 40-gm nylon mesh to remove clumps of cells and connective tissue. After two times wash of PBS the cell suspension was adjusted to final concentration of 5×10^5 cells/mL RPMI-1640 with 10% FCS in 96-well microtiter plates, and the blastogenic assays were carried out with 0.2 mL of suspensions. Cell viability was tested by use of fluoresce diacetate. The cultures of splenocyte cells were at 37 °C incubated with mitogen concanavalin A (Con-A, 5×10^{-5} M) and 5% CO_2 for 48 h, and the cells received MTT assay to calculate the relative spleen lymphocyte proliferation (%) according to proliferation% = (ODT - ODC) / ODC × 100%, wherein ODT refers the absorbance of MTCTP5 and ODC refers the absorbance of RPMI-1640 (blank control).

Plasma TNF-α assay on S180 mice

In the preparation of the plasma sample 0.9 mL of blood collected from health mice or S180 mice receiving MTCTP5 (2, 0.2, 0.02 μmol/kg) or NS into a syringe containing 0.1 mL of 3.8% sodium citrate. Sample was centrifuged at 4 °C and 3000 rpm for 10 min to prepare plasma sample. To each of three blank wells nothing was added. To each of six standard wells 100μL standard solution was added. To each of three testing wells 100 μL plasma sample from health mice or the mice receiving NS or MTCTP5 (2, 0.2, 0.02 μmol/kg) was added. Then the plate was closed with closure plate membrane and at 37 °C incubated for 40 min. On uncovering the closure plate membrane the well was discarded the liquid and dried by swing, to the residue in the well sufficient washing buffer, which was prepared by diluting the wash solution with 30 folds distilled water, was added, stilled for 30 s, and then drained. After 5 time repeats of the procedure, 50 μL Biotinylated Antibody solution and 50 μL distilled water was added, then the plate was closed with closure plate membrane and at 37 °C incubated for 30 min. On uncovering the closure plate membrane the well was discarded the liquid and washed by sufficient washing buffer for 5 times. After 5 time repeats of the procedure, 100 μL Biotinylated Antibody solution was added and the plate was closed with closure plate membrane and at 37 °C incubated for 30 min. On uncovering the closure plate membrane the well was discarded the liquid and washed by sufficient washing buffer for 5 times and dried by pat. To the residue in the well 50 μL chromogen solution A and 50 μL chromogen solution B were added, gently mixed and at 37 °C and protecting from light incubated for 10 min. To each well 50 μL stop solution was added, and the color in the well changed from blue to yellow. The plate was read at 450 nm using a microtiter plate reader within 15 min to record O.D. value. According to the standard curve the concentrations of TNF-α in plasma were calculated.

Plasma IL-8 assay on S180 mice

In the preparation of the plasma sample 0.9 mL of blood collected from health mice or S180 mice receiving MTCTP5 (2, 0.2, 0.02 μmol/kg) or NS into a syringe containing 0.1 mL of 3.8% sodium citrate. Sample was centrifuged at 4 °C and 3000 rpm for 10 min to prepare plasma sample. To each of three blank wells nothing was added. To each of six standard wells 100 μL standard solution was added. To each of three testing wells 100 μL plasma sample from health mice or the mice receiving NS or MTCTP5 (2, 0.2, 0.02 μmol/kg) was added. Then the plate was closed with closure plate membrane and at 37 °C incubated for 40 min. On uncovering the closure plate membrane the well was discarded the liquid and dried by swing, to the residue in the well sufficient washing buffer, which was prepared by diluting the wash solution with 30 folds distilled water, was added, stilled for 30 s, and then drained. After 5 time repeats of the procedure, 50 μL Biotinylated Antibody solution and 50 μL distilled water was added, then the plate was closed with closure plate membrane and at 37 °C

incubated for 30 min. On uncovering the closure plate membrane the well was discarded the liquid and washed by sufficient washing buffer for 5 times. After 5 time repeats of the procedure, 100 μL Biotinylated Antibody solution was added and the plate was closed with closure plate membrane and at 37 °C incubated for 30 min. On uncovering the closure plate membrane the well was discarded the liquid and washed by sufficient washing buffer for 5 times and dried by pat. To the residue in the well 50 μL chromogen solution A and 50 μL chromogen solution B were added, gently mixed and at 37 °C and protecting from light incubated for 10 min. To each well 50 μL stop solution was added, and the colour in the well changed from blue to yellow. The plate was read at 450 nm using a microtiter plate reader within 15 min to record O.D. value. According to the standard curve the concentrations of IL-8 in plasma were calculated.

Lifespan assay

Lifespan assay was performed by using a standard procedure. In brief, male ICR mice were 10-12 weeks old at the beginning of experiments. S180 cells for initiation of subcutaneous tumors were obtained from the ascitic form of the tumors in mice, which were serially transplanted once per week. Subcutaneous tumors were implanted by injecting 0.2 mL NS containing 1×10^7 viable tumor cells under the skin on right oxter. Twenty four hours after implantation the tumor bearing mice were randomized into 4 experimental groups (12 per group). All mice were given a daily intraperitoneal injection of TP5 (2 μmol/kg/day in NS) or MTC (2 μmol/kg/day in NS) or NS (10 mL/kg/day) or MTCTP5 (2 μmol/kg/day in NS) for 33 consecutive days. Mouse death due to tumor burden was noted and the lifespan was calculated as [(T-C)/C]%, wherein T and C represent survival days of treated and untreated mice, respectively.

Plasma ALT and AST assays

0.9 mL blood of the mice receiving anti-tumor assay was collected into a syringe containing 0.1 mL of 3.8% sodium citrate and immediately centrifuged at 3000 rpm for 10 minutes to get the plasma samples. The separated plasma was used to measure plasma levels of alanine transaminase (ALT) and aspartate transaminase (AST) according to the guidance of the kits (AST/GOT testing kit, ALT/GPT testing kit; JCBIO Co., Nanjing, People's Republic of China). In brief 5 μL of plasma was add into the test wells of 96 microtiter plates, and then adding 20 μL Matrix liquid and incubated at 37 ºC for 30 min, 5 μL of plasma was add into the control wells of 96 microtiter plates, and 20 μL of 2,4-dinitrophenylhydrazinewas added to all wells, incubated at 37 ºC for 20 min, 200 μL 0.4 mol/L NaOH was added, incubated at 37 ºC for 15 min, and the absorbance of the yellow solutions were recorded at 510 nm to calculate vitality based on $(OD_{test} - OD_{control}) \times K_{curve}$, wherein OD_{test} referred to absorbance of test well and $OD_{control}$ referred to absorbance of control well, the K_{curve} referred to standard curve which calculated by absorbance of standard well following the manufacturer's protocols.

Plasma Cr assay

0.9 mL blood of the mice receiving anti-tumor assay was collected into a syringe containing 0.1 mL of 3.8% sodium citrate and immediately centrifuged at 3000 rpm for 10 minutes to get the plasma samples. The separated plasma was used to measure plasma levels of creatinine (Cr) according to the guidance of the kits (Cr testing kit; JCBIO Co., Nanjing, People's Republic of China). In brief 6 μL of plasma or standard solution was added into the wells of 96 microtiter plates, 180 μL of the enzyme solution A was added to incubate at 37 ºC for 5 min, and 60 μL of the enzyme solution B was added to incubate at 37 ºC for 5 min, and the absorbance of the purple solutions were recorded at 546 nm to calculate vitality based on $(OD_{test} - OD_{control}) \times K_{curve}$, wherein OD_{test} refers absorbance of test well, $OD_{control}$ refers absorbance of control well and K_{curve} refers standard curve.

Results and discussion

1. Synthesis and structural characterization

1.1. Preparation and chemical structure of MTCTP5

MTC (**2**) and the intermediates (**3**-**5**) were prepared by following the previous procedure.[39,40] TP5 and the intermediates were prepared by following the general route.[41-43]

As depicted in Scheme 1 MTCTP5 was prepared via 12-step reactions, the yields ranged from 63% to 99% and the total yield was 5.6%. The ^{1}H NMR, ^{13}C NMR, FT-MS and IR spectra are given as Figures S1-S8 of the Supporting Information, which supports MTCTP5 having correct chemical structure.

1.2. Nanofeature and size of MTCTP5

The nanofeature and size of MTCTP5 in water, in solid state and in mouse plasma were described with TEM, SEM and AMF images, respectively.

TEM images (Figure 1A) indicate that when the powders of MTCTP5 are dissolved in ultrapure water to form a solution of 10^{-7} nM MTCTP5 can form the nanoparticles of 30-110 nm in diameter. The insert indicates that in the amplified nanoparticle 7 small particles are included and on the surface of the amplified nanoparticle numerous holes of ~7 nm in diameter are observed.

SEM images (Figure 1B) indicate that the solids resulted from 10^{-7} nM solution of MTCTP5 in ultrapure water are equally distributed nanoparticles of 10-92 nm in diameter, for most nanoparticles the diameter is less than 50 nm.

AFM images (Figure 1C) indicates that in mouse plasma MTCTP5 (final concentration, 10^{-7} nM) forms nanoparticles of 14-139 nm in diameter, for most nanoparticles the diameter is less than 100 nm, and some nanoparticles can form aggregators.

On the other hand no any comparable nanoparticle is found in the AFM image of mouse plasma alone (Figure 1D).

The DLS determinations of 7 consecutive days explored that in ultrapure water the nano-size of MTCTP5 ranged from 186 nm to 320 nm in diameter. These data imply that the nanoparticles' diameter of MTCTP5 in water increases slightly in 7 days. (Figure 1E)

The zeta-potential determinations explored that in ultrapure water and in mouse plasma the zeta-potentials of MTCTP5 were -8.56 ± 0.89 mV and -25.13 ± 0.98 mV, respectively. These data imply that the nanoparticles' diameter of MTCTP5 in ultrapure water is larger than that of MTCTP5 in mouse plasma, and this should benefit the delivery of the nanoparticles in blood circulation.

2. Bioactivity related to MTC moiety of MTCTP5

2.1 *In vivo* anti-tumor activity of MTCTP5

The anti-tumor activity of MTCTP5 was examined with S180 tumor bearing mouse assay and represented with tumor weight. Figure 2A indicates that the tumor weights of the mice intraperitoneally receiving 2 μmol/kg of MTC and 0.02 μmol/kg of MTCTP5 are significantly lower than that of the mice intraperitoneally receiving NS, while the tumor weight of the mice intraperitoneally receiving 0.2 μmol/kg of MTCTP5 is equal to that of the mice intraperitoneally receiving 2 μmol/kg of Dox.

2.2. *In vivo* anti-thrombotic activity of MTCTP5

The anti-thrombotic activity of MTCTP5 was examined with rat thrombosis assay and represented with thrombus weight. Figure 2B indicates that the thrombus weights of the rats receiving 2 μmol/kg of MTC is significantly lower than that of the rats receiving NS, suggesting at 2 μmol/kg of dose MTC can inhibit the rats to form thrombus. Figure 2B also indicates that the thrombus weight of the rats receiving 2 μmol/kg of MTC is significantly higher than that of the rats receiving 0.2 μmol/kg of MTCTP5, while the thrombus weight of the rats receiving 2 μmol/kg of MTCTP5 is equal to that of the rats receiving 167 μmol/kg of aspirin.

2.3. *In vivo* anti-inflammation activity of MTCTP5

The anti-inflammation activity of MTCTP5 was examined with xylene-induced ear edema assay. Figure 2C indicates that the anti-inflammation activity of 2 μmol/kg of MTC is significantly higher than that of NS and is equal to that of 0.02 μmol/kg of MTCTP5. Besides, the anti-inflammation activity of 0.2 μmol/kg of MTCTP5 is equal to that of 1100 μmol/kg of aspirin.

3. Bioactivity related to TP5 moiety of MTCTP5

3.1. Proliferation of splenocyte cells treated with MTCTP5

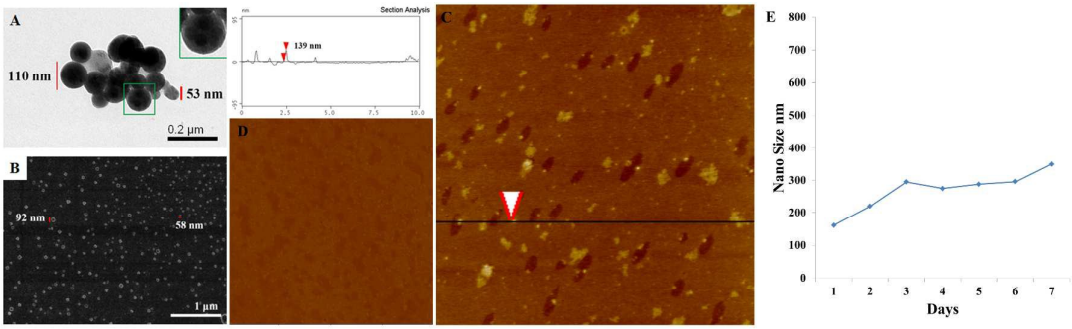

Figure 1 Nanofeature and size of MTCTP5. (A) TEM image of MTCTP5 in ultrapure water (10^{-7} nM); (B) SEM image of the solids from a solution of MTCTP5 in ultrapure water (10^{-7} nM); (C) AFM image of MTCTP5 in mouse plasma (10^{-7} nM); (D) AFM image of mouse plasma alone; (E) The change of nano-size of MTCTP5 in ultrapure water within 7 days.

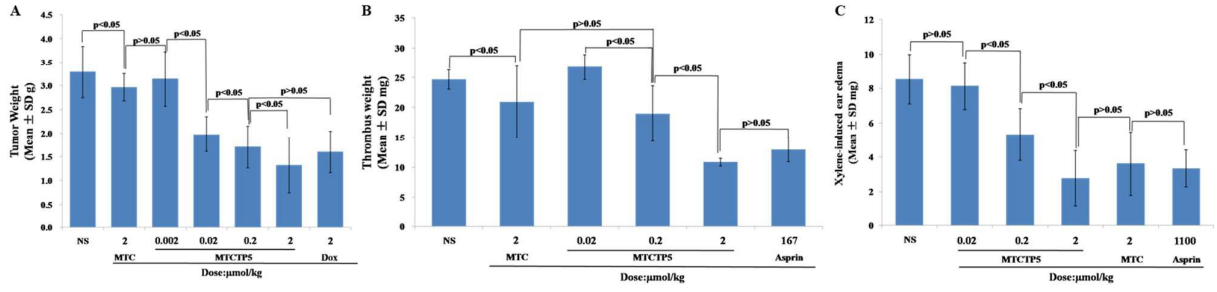

Figure 2 *In vivo* anti-tumor, anti-thrombotic and anti-inflammatory activities of MTCTP5. (A) At 0.002 μmol/kg of dose MTCTP5 effectively allows the tumor growth of S180 mice; (B) At 0.2 μmol/kg of dose MTCTP5 effectively inhibits the rats to form thrombus; (C) At 0.2 μmol/kg of dose MTCTP5 effectively inhibits xylene inducing the mice to develop ear edema; n = 12.

The immunologic enhancing activity related to TP5 moiety was tested with the *in vitro* proliferation of splenocyte cells treated with MTCTP5. Figure 3A indicates that the proliferation of splenocyte cells treated with 50 μM of ConA plus 100 μM of TP5 is equal to that of splenocyte cells treated with 50 μM of ConA plus 100 μM of MTCTP5, and is significantly higher than that of splenocyte cells treated with 50 μM of ConA alone.

3.2. *In vivo* phagocytosis index of MTCTP5 treated ICR mice

The immunologic enhancing activity related to TP5 moiety was further tested with carbon clearance assay and is represented with phagocytosis index of MTCTP5 treated ICR mice. Figure 3B indicates that the phagocytosis index of ICR mice treated with 2 μmol/kg of MTCTP5 is equal to that of ICR mice treated with 2 μmol/kg of TP5, and is significantly higher than that of ICR mice treated with NS.

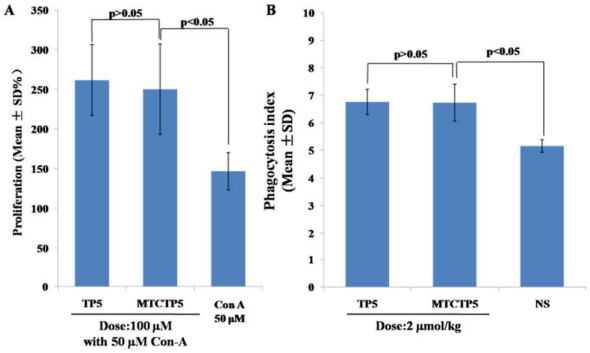

Figure 3 The immunologic enhancing activities of MTCTP5. (A) Effect of MTCTP5 on the *in vitro* proliferation of splenocyte cells, n = 6; (B) Effect of MTCTP5 on phagocytosis index of MTCTP5 treated ICR mice, n = 10.

4. Effect of MTCTP5 on TNF-α, IL-8, IL-2, CD4 and CD8 of the treated mice

4.1. Effect of MTCTP5 on plasma TNF-α of the treated mice

To explore the action mechanism of MTCTP5 inhibiting thrombosis, inflammation and tumor growth the plasma TNF-α of MTCTP5 treated S180 mice was tested. The data of Figure 4A indicates that the plasma TNF-α of 2 and 0.2 μmol/kg of MTCTP5 treated S180 mice are significantly lower than that of NS treated S180 mice, while the plasma TNF-α of 0.02 μmol/kg of MTCTP5 treated S180 mice is equal to that of NS treated S180 mice.

4.2. Effect of MTCTP5 on IL-8 of the treated mice

To explore the action mechanism of MTCTP5 inhibiting thrombosis, inflammation and tumor growth the plasma IL-8 of MTCTP5 treated S180 mice was also tested. The data of Figure 4B indicates that the plasma IL-8 of 2 and 0.2 μmol/kg of MTCTP5 treated S180 mice are significantly lower than that of NS treated S180 mice, while the plasma IL-8 of 0.02 μmol/kg of MTCTP5 treated S180 mice is equal to that of NS treated

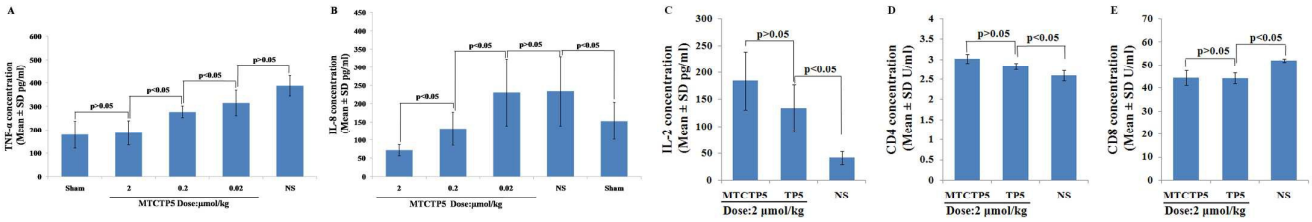

Figure 4 Effect of MTCTP5 on TNF-α and IL-8. (A) Plasma TNF-α of MTCTP5 treated S180 mice, n = 12; (B) Plasma IL-8 of MTCTP5 treated S180 mice, n = 12; (C) Peripheral blood IL-2 of MTCTP5 treated ICR mice, n = 10; (D) Peripheral blood CD4 of MTCTP5 treated ICR mice, n = 10; (E) Peripheral blood CD8 of MTCTP5 treated ICR mice, n = 10.

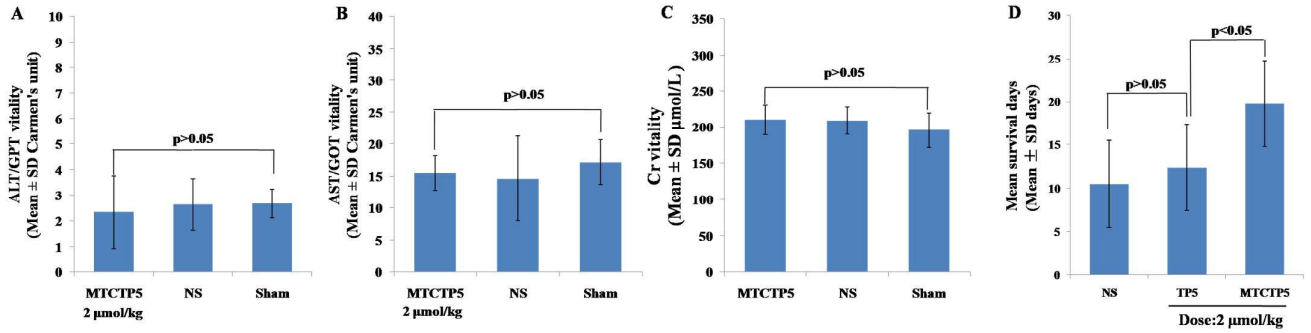

Figure 5 Plasma ALT, AST and Cr, as well as survival time of the mice treated with MTCTP5.(A) Plasma ALT of the mice treated with MTCTP5, n = 12; (B) Plasma AST of the mice treated with MTCTP5, n = 12; (C) Plasma Cr of the mice treated with MTCTP5, n = 12; (D) Survival time of the mice treated with MTCTP5, n = 12.

S180 mice.

4.3. Plasma IL-2, CD4 and CD8 of MTCTP5 treated ICR mice

The immunologic enhancing activities related to TP5 moiety of MTCTP5 was tested with plasma IL-2, CD4 and CD8 assays *in vivo*. Figures 4C-4E indicate that the plasma IL-2 and CD4 of 2 μmol/kg of MTCTP5 treated ICR mice are equal to those of 2 μmol/kg of TP5 treated ICR mice and are significantly higher than those of NS treated ICR mice, meanwhile CD8 of 2 μmol/kg of MTCTP5 treated ICR mice is equal to that of 2 μmol/kg of TP5 treated ICR mice and is significantly lower than that of NS treated ICR mice.

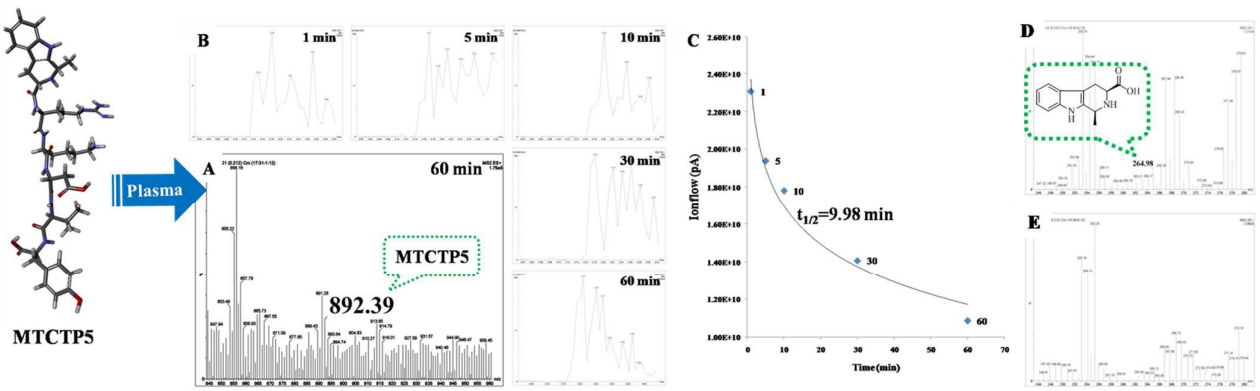

Figure 6 ESI-MS spectra, total ion current chromatogram/time course of MTCTP5 in mouse plasma. (A) ESI(+)-MS spectrum of MTCTP5 in mouse plasma been incubated for 60 min; (B) Total ion current chromatograms of MTCTP5 in mouse plasma been incubated for 1, 5, 10, 30 and 60 min; (C) Area of total ion current chromatogram of MTCTP5 in mouse plasma been incubated for 1, 5, 10, 30 and 60 min; (D) ESI(-)-MS spectrum of MTCTP5 in mouse plasma been incubated for 30 min and the ion peak of MTC; (E) ESI(-)-MS spectrum of mouse plasma alone been incubated for 30 min.

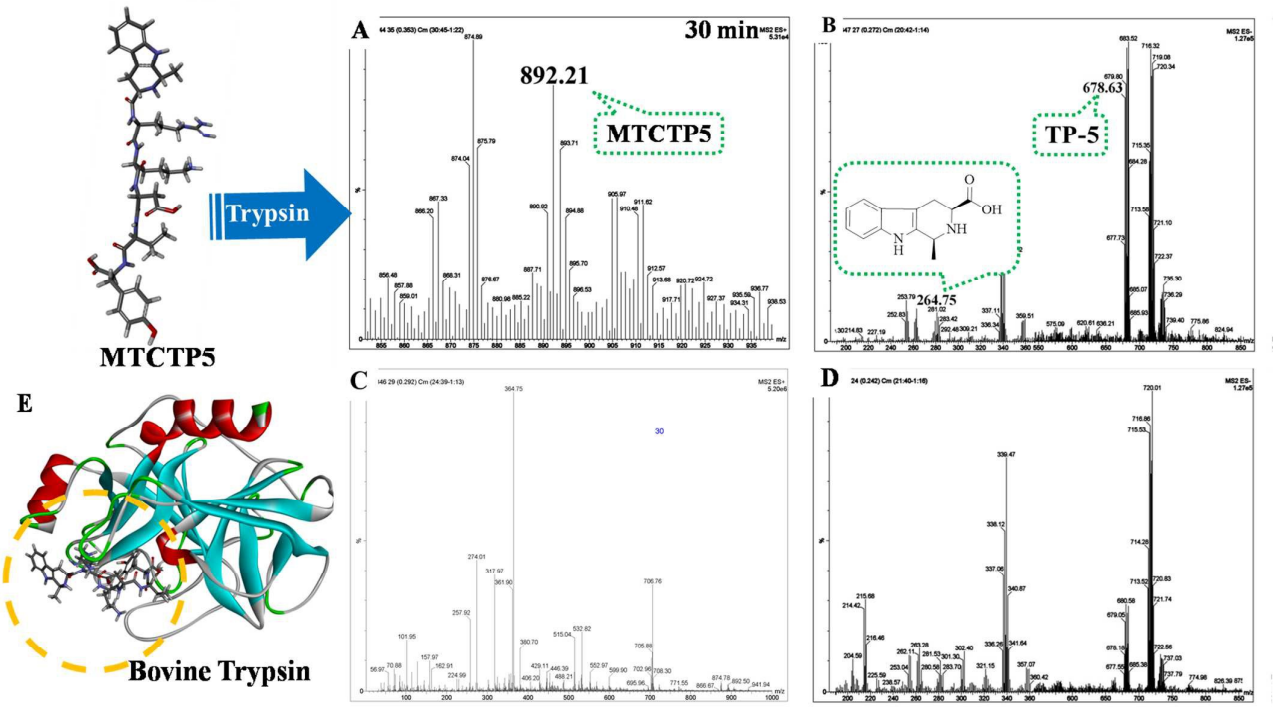

Figure 7 ESI-MS spectra of MTCTP5 in presence of trypsin. (A) ESI(+)-MS spectrum of MTCTP5 in presence of trypsin at 37 ºC been incubated for 30 min; (B) Locally amplified ESI(-)-MS spectrum of MTCTP5 in presence of trypsin at 37 ºC been incubated for 30 min; (C) ESI(+)-MS spectrum of MTCTP5 in presence of trypsin at 37 ºC been incubated for 30 min; (D) Locally amplified ESI(-)-MS spectrum of trypsin alone at 37 ºC been incubated for 30 min.

5. Toxicity of MTCTP5

5.1. Plasma ALT of MTCTP5 treated S180 mice

The hepatotoxicity of MTCTP5 was examined with plasma alanine transaminase (ALT) assay. In brief, the blood from the mice receiving *in vivo* antitumor assay was collected to obtain the plasma. The plasma ALT was measured according to the guidance of the kit, and the data are shown in Figure 5A. Plasma ALT of the sham mice, the NS treated mice and 2 μmol/kg of MTCTP5 treated mice exhibit no significant difference.

5.2. Plasma AST of MTCTP5 treated S180 mice

The hepatotoxicity of MTCTP5 was also examined with plasma aspartate transaminase (AST) assay. In brief, the blood of the mice receiving *in vivo* antitumor assay was collected to obtain the plasma. The plasma AST was measured according to the guidance of the kit, and the data are shown in Figure 5B. Plasma AST of sham mice, of NS treated mice and of 2 μmol/kg of MTCTP5 treated mice exhibit no significant difference.

5.3. Plasma Cr of MTCTP5 treated S180 mice

The renal toxicity of MTCTP5 was examined with plasma creatinine (Cr) assay. In brief, the blood from the mice receiving *in vivo* antitumor assay was collected to obtain the plasma. The plasma Cr was measured according to the guidance of the kit, and the data are shown in Figure 5C. The plasma Cr of sham mice, of NS treated mice and of 2 μmol/kg of MTCTP5 treated mice exhibit no significant difference.

5.4. Survival time of MTCTP5 treated S180 mice

The systemic toxic action of MTCTP5 was firstly examined with vital stage of S180 tumor bearing mouse assay and represented with the survival time. Figure 5D indicates that the survival time of NS treated mice is equal to that of 2 μmol/kg TP5 treated mice. Figure 5D also indicates that the survival time of 2 μmol/kg MCTP5 treated mice is significantly longer than those of NS and 2 μmol/kg TP5 treated mice.

6. MTCTP5 releasing MTC and/or TP5

6.1. MTCTP5 releasing MTC in mouse plasma

To explore the release profile 1 mg of MTCTP5 was in 1 mL of mouse plasma at 37 ºC incubated for 10, 20, 30, 60 and 90 min, and the plasma samples were extracted with ultrapure water for ESI-MS analysis. Figure 6A indicates that 60 min after the incubation the ESI(+)-MS spectrum of the extract gives an ion peak at 892.39 of the molecule of MTCTP5 plus H, $[M + H]^+$ (exact mass: 892.46). Figure 6B shows the total ion current chromatograms of 1 mg of MTCTP5 in 1 mL of mouse plasma at 37 ºC been incubated for 1, 5, 10, 30 and 60 min, and suggests that in 37 ºC mouse plasma MTCTP5 can stably exist for more than 60 min. Figure 6C plots the incubation time *vs* the area of total ion current chromatogram, and suggests that in 37 ºC mouse plasma MTCTP5 has a half-life of 9.98 min. Figure 6D shows the ESI(-)-MS spectrum of MTCTP5 in mouse plasma at 37 ºC been incubated for 30 min, and gives the ion peak at 264.98 of the molecule of MTC plus Cl, $[M + Cl]^-$ (exact mass: 265.07). Figure 6E shows the ESI(-)-MS spectrum of mouse plasma alone at 37 ºC bee incubated for 30 min, and gives no such a peak.

6.2. MTCTP5 releasing MTC and TP5 in trypsin

To estimate the release profile of MTCTP5 in presence of trypsin a solution of 1 mg of MTCTP5 and 800 IU of trypsin in 1 mL of ultrapure water was at 37 ºC incubated for 30 min, of which the ESI(+/-)-MS spectra are shown in Figure 7. The locally amplified ESI(+)-MS spectrum between 800-900 gives a peak of molecular ion of MTCTP5 plus H at 892.21, $[M + H]^+$ (exact mass: 892.46, Figure 7A). The locally amplified ESI(-)-MS spectrum between 200-850 gives a peak of molecular ion of MTC plus Cl at 264.75, $[M + Cl]^+$ (exact mass: 265.07), and a peak of molecular ion of TP5 minus H at 678.63, $[M -H]^-$ (exact mass: 678.36, Figure 7B). The total ESI(+)-MS spectrum of a solution of 1 mg of MTCTP5 and 800 IU of trypsin in 1 mL of ultrapure water been incubated at 37 ºC for 30 min is shown with Figure 7C. Figure 7D shows the locally amplified ESI(-)-MS spectrum between 200-850 of 800 IU of trypsin in 1 mL of ultrapure water been incubated at 37 ºC for 30 min, and gives no comparable ion peaks of MTC plus Cl and TP5 minus H.

To explain the molecular mechanism of trypsin promoting MTCTP5 to release MTC and TP5, MTCTP5 was docked into the active site of bovine trypsin (Figure 7E). It was found that MTCTP5 well fitted the active site, and well interacted with the amino acid residues of the active site.

Discussion

Using the synthetic route MTCTP5 can be successfully prepared in acceptable yield and desirable purity. In water the molecular association leads MTCTP5 to form trimers. qCID spectrum suggests that in the condition of FT-MS fragmentation the trimer directly forms the monomer, no any dimer could be monitored. Three interesting cross-peaks of the NOESY 2D NMR spectrum define the association manner of 3 molecules in forming the trimer. Due to the distances between two H of across-peak is less than 4Å, thus to form a trimer three molecules of MTCTP5 have to approach in the manner of Figure S10A,B and should take flyer-like conformation of Figure S10C.

The images of TEM, SEM and AFM explore that the self-assembly of the trimers leads MTCTP5 to spontaneously forming nanoparticles. The proper size of 14-139 nm in diameter benefits the delivering of the nanoparticles in blood circulation. The zeta potentials of the nanoparticles of MTCTP5 in water and mouse plasma are -8.56 ± 0.89 mV and -25.13 ± 0.98 mV, respectively, and support the stability of the

nanoparticles.

The anti-tumor assay indicates that the tumor weight of the mice treated with 0.02 μmol/kg of MTCTP5 is significantly lower than those of the mice treated with both 2 μmol/kg of MTC and NS, suggesting the minimal effective dose of MTCTP5 in treating tumor is 0.02 μmol/kg, and the conjugation of TP5 with MTC leads the anti-tumor activity of MTC to an increase of 100 folds. Besides, the tumor weight of the mice treated with 0.2 μmol/kg of MTCTP5 is equal to that of the mice treated with 2 μmol/kg of Dox, meaning the activity of MTCTP5 is 10 folds higher than that of Dox. It is worthy of indicating that in the *in vitro* MTT assay the IC_{50} of MTCTP5 against K562, A549, HT-29 and HL-60 cells are higher than 150 μM, suggesting the anti-tumor action of MTCTP5 *in vivo* is independent of the cytotoxic action.

The anti-thrombotic assay indicates that the thrombus weight of the rats receiving 0.2 μmol/kg of MTCTP5 is significantly lower than those of the rats receiving 2 μmol/kg of MTC and NS, meaning the minimal effective dose of MTCTP5 in treating thrombus is 0.2 μmol/kg as well as the conjugation of TP5 and MTC leads the anti-thrombotic activity of MTC to an increase of >10 folds. Besides, the thrombus weight of the rats receiving 2 μmol/kg of MTCTP5 is equal to that of the rats receiving 167 μmol/kg of aspirin, suggesting the anti-thrombotic activity of MTCTP5 is 83.5 folds higher than that of aspirin.

The anti-inflammatory assay indicates that xylene-induced ear edema of the mice treated with 0.2 μmol/kg of MTCTP5 is significantly lower than that of the mice treated with NS, suggesting the minimal effective dose of MTCTP5 in treating inflammation is 0.2 μmol/kg. Xylene-induced ear edema of the mice treated with of 0.2 μmol/kg of MTCTP5 is equal to that of the mice treated with 2 μmol/kg of MTC, suggesting the conjugation of TP5 and MTC leads the anti-inflammatory activity of MTC to an increase of 10 folds. Besides, xylene-induced ear edema of the mice treated with of 2 μmol/kg of MTCTP5 is equal to that of the mice treated with 1100 μmol/kg of aspirin, i.e. the anti-inflammatory activity of MTCTP5 is 550 folds higher than that of aspirin.

Chronic inflammation is recently correlated with thromboembolism,[44] which are well documented as the commonly encountered implications of cancer patients.[45,46] The facts that at 0.2 μmol/kg of dose MTCTP5 simultaneously slows tumor growth, inhibits thrombosis and depresses inflammation demonstrate that MTCTP5 is a promising lead compound for treating cancer patients without complicating chronic inflammation and thromboembolism.

Splenocyte cell proliferation assay indicates that for ConA treated splenocyte cells the enhanced proliferations of 100 μM of TP5 and 100 μM of MTCTP5 are the same, suggesting the conjugation of MTC with TP5 does not weaken the *in vitro* immunologic enhancing activity of TP5. Carbon clearance assay indicates that at 2 μmol/kg of dose the phagocytosis index of TP5 and MTCTP5 treated mice are the same and significantly higher than that of NS treated mice, suggesting the conjugation of MTC with TP5 does not weaken the *in vivo* immunologic enhancing activity of TP5.

The plasma TNF-α and IL-8 levels of 2, 0.2 and 0.02 μmol/kg of MTCTP5 treated S180 mice indicate that MTCTP5 down regulates the plasma levels of TNF-α and IL-8 of S180 mice in a dose-dependent manner. The significantly different plasma levels of TNF-α and IL-8 of 0.2μmol/kg of MTCTP5 and NS treated S180 mice indicate that the minimal effective dose of MTCTP5 down regulating plasma levels of TNF-α and IL-8 of S180 mice is 0.2μmol/kg. The plasma levels of TNF-α and IL-8 of 2 μmol/kg of MTCTP5 treated S180 mice and the sham mice are the same indicate that at 2 μmol/kg of dose MTCTP5 can resume the plasma TNF-α and IL-8 of S180 mice to normal level. Due to plasma TNF-α and IL-8 are considered the biomarker of tumor, thrombus and inflammation, MTCTP5 dose-dependently down-regulates plasma levels of TNF-α and IL-8 of S180 mice would be responsible for it simultaneously inhibiting tumor growth, thrombus formation and inflammatory response.

The plasma IL-2 and CD4 levels of 2 μmol/kg of MTCTP5 and 2 μmol/kg of TP5 treated S180 mice are the same and significantly lower than those of NS treated S180 mice, while the CD8 levels of 2 μmol/kg of MTCTP5 and 2 μmol/kg of TP5 treated S180 mice are the same and significantly lower than that of NS treated S180 mice indicate that MTC conjugating TP5 does not change the immunologic enhancing action of TP5. Due to plasma IL-2, CD4 and CD8 are considered the biomarker of immunomodulation, MTCTP5 regulates plasma levels of IL-2, CD4 and CD8 would be responsible for its immunologic enhancing activity.

The quantitative release of MTC from MTCTP5 was confirmed with the total ion current chromatograms of ESI(+)-MS spectra of the aqueous extracts of MTCTP5 in mouse plasma at 37 ºC incubated for 10, 20, 30, 60 and 90 min. The results not only support that in blood circulation MTCTP5 can release MTC, thereby inhibit tumor growth, thrombus formation and inflammatory response, but also give MTCTP5 a half-life of 9.98 min. Comparing to TP5 (half-life, ~9 s) the half-life of MTCTP5 is ~60 folds longer, and this should be responsible for the enhanced bioactivities of MTCTP5.

Even though ESI(+/-)-MS spectra of the aqueous extracts fail to give the ion peak of TP5, the ESI(-)-MS spectrum of the incubation sample of MTCTP5 in presence of trypsin gives both the ion peaks of MTC and TP5. Thus we hypothesize that MTCTP5 should be a nanomedicine capable of releasing MTC and TP5.

Conclusions

The nano-scale conjugate of TP5 and MTC (MTCTP5) is a novel delivery system for TP5 and MTC. In 37 °C plasma MTCTP5 can exist for at least 60 min and can release MTC and

TP5. Comparing to MTC, MTCTP5 possesses significant higher anti-inflammatory, anti-thrombotic and anti-tumor activities. Comparing to TP5, MTCTP5 possesses similar immunologic enhancing activity. Besides, MTCTP5 minimally injures the liver and kidney. The proper nano-structure, the potent efficacy, the minimal toxic action, and the correlations of the bioactivities with IL-8, THF-α, IL-2, CD4 and CD8 demonstrate that MTCTP5 would be a promising nanomedicine.

Acknowledgements

This work was supported by Beijing Municipal Science & Technology Commission (Z141100002114049), PXM2013014226000002, TJSHG (201310025008), IHLB (KZ201210025021), 863 program (AA2015020902), Beijing Nova programme XX2013039, National Natural Science Foundation (81172930, 81273379, 81373264, 81373265 and 81270046) and Beijing Natural Science Foundation (7132032).

Notes and references

1 V. K. Singh, S. Biswas, K. B. Mathur, W. Haq, S. K. Garg, and S. S. Agarwal, *Immunologic research*, 1998, **17**, 345.
2 Y. J. Hoshida, B. C. Fuchs, and K. K. Tanabe, *Curr Cancer Drug Targets.*, 2012, **12**, 1129.
3 J. Cukuranovic, S. Ugrenovic, I. Jovanovic, M. Visnjic and V. Stefanovic, *ScientificWorldJournal.*, 2012, **2012**, 820621.
4 T. K. Audhya and G. Goldstein, *Survey of immunologic research*, 1985, **4**, 17.
5 Y. Wang, X. Y. Ke, J. S. Khara, P. Bahety, S. Q. Liu, S. V. Seowc, Y. Y. Yang and P. L. R. Ee , *Biomaterials.*, 2014, **35**, 3102.
6 X. Z. Lao, B. Li, M. Liu, J. Chen, X. D. Gao and H. Zheng, *Biochimie*, 2014, **107**, 277.
7 J. Li, Y. Cheng, X. K. Zhang, L. Zheng, Z. Han, P. L. Li, Y. L. Xiao, Q. Zhang and F. S. Wang, *Cancer Lett.*, 2013, **337**, 237
8 X. F. Jin, Y. Xu, J. Shen, Q. N. Ping, Z. G. Su and W. L. You, *Carbohydr. Polym.*, 2011, **86**, 51.
9 Y. S. Yin, D. W. Chen, M. X. Qiao, Z. Lu and H. Y. Hu, *J. Controlled Release*, 2006, **116**, 337.
10 J. Wang, W. L. Lu, G. W. Liang, K. C. Wua, C. G. Zhang, X. Zhang, J. C. Wang, H. Zhang, X. Q. Wang and Q. Zhang, *Peptides*, 2006, **27**, 826.
11 L. Wang, Y. Zhang and X. Tang, *Int. J. Pharm.*, 2009, **375**, 1.
12 Y. Zhang, X. H. Wua, Y. R. Han, F. Mo, Y. R. Duan and S. M. Li, *Int. J. Pharm.*, 2010, **386**, 15.
13 Y. H. Tan, Z. W. Yang, X. Pan, M. W. Chen, M. Feng, L. L. Wang, H. Liu, Z. Y. Shan and C. B. Wua, *Int. J. Pharm.*, 2012, **427**, 385.
14 B. Conti, A. M. Panico, C. A. Ventura, P. Giunchedi, and G. Puglisi, *J. Microencapsulation*, 1997, **14**, 303.
15 J. H. Im, Y. R. Jin, J. J. Lee, J. Y. Yu, X. H. Han, S. H. Im, J. T. Hong, H. S. Yoo, M. Y. Pyo and Y. P. Yun, *VasculPharmacol.*, 2009, **50**, 147.
16 D. J. Moura, C. Rorig, D. L. Vieira, J. A. P. Henriques, R. Roesler, J. Saffi and J. M. Boeira, *Life Sci.*, 2006, **79**, 2099.
17 R. H. Bahekar, M. R. Jain, P. A. Jadav, A. Goel, D. N. Patel, V. M. Prajapati, A. A. Gupta, H. Modi and P. R. Patel, *Bioorg. Med. Chem.*, 2007, **15**, 5950.
18 L. C. Tu, C. S. Chen, I. C. Hsiao, J. W. Chern, C. H. Lin, Y. C. Shen and S. F. Yeh, *Chem. Biol.*, 2005, **12**, 1317.
19 L. S. Santos, C. Theoduloz, R. A. Pilli and J. Rodriguez, *Eur. J. Med. Chem.*, 2009, **44**, 3810.
20 R. H. Valdeza, L. T. D. Tonin, T. Ueda-Nakamura, B. P. D. Filho, J. A. Morgado-Diazd, M. H. Sarragiotto and C. V. Nakamura, *Acta Trop.*, 2009, **110**, 7.
21 L. Gupta, K. Srivastava, S. Singh, S. K. Puri and P. M. S. Chauhan, *Bioorg. Med. Chem. Lett.*, 2008, **18**, 3306.
22 K. Takasu, T. Shimogama, C. Saiin, H. S. Kim, Y. Wataya and M. Ihara, *Bioorg. Med. Chem. Lett.*, 2004, **14**, 1689.
23 R. Cao, W. Peng, H. Chen, X. Hou, H. Guan, Q. Chen, Y. Ma and A. Xu, *Eur. J. Med. Chem.*, 2005, **40**, 249.
24 J. Hamann, C. Wernicke, J. Lehmann, H. Reichmann, H. Rommelspacher and G. Gille, *Neurochem. Int.*, 2008, **52**, 688.
25 A. S. N. Formagio, P. R. Santos, K. Zanoli, T. Ueda-Nakamura, L. T. D. Tonin, C. V. Nakamura and M. H. Sarragiotto, *Eur. J. Med. Chem.*, 2009, **44**, 4695.
26 S. Manda, S. I. Khan, S. K. Jain, S. Mohammed, B. L. Tekwani, I. A. Khan, R. A. Vishwakarma and S. B. Bharate, *Bioorg. Med. Chem. Lett.*, 2014, **24**, 3247.
27 R. Cao, W. Peng, H. Chen, X. Hou, H. Guan, Q. Chen, Y. Ma, and A. Xu, *Eur J Med Chem.*, 2005, **40**, 249.
28 R. Cao, Q. Chen, X. Hou, H. Chen, H. Guan, Y. Ma, W. Peng and A. Xu, *Bioorg. Med. Chem.*, 2004, **12**, 4613.
29 R. Cao, H. Chen, W. Peng, Y. Ma, X. Hou, H. Guan, X. Liu and A. Xu, *Eur. J. Med. Chem.*, 2005, **4**, 991.
30 B. Baruah, K. Dasu, B. Vaitilingam, P. Mamnoor, P. P. Venkata, S. Rajagopal and K. R. Yeleswarapu, *Bioorg. Med. Chem.*, 2004, **12**, 1991.
31 L. Zeng and J. Zhang, *Bioorg. Med. Chem. Lett.*, 2012, **22**, 3718.
32 K. Yao, M. Zhao, X. Y. Zhang, Y. J. Wang, L. Li, M. Q. Zheng and S. Q. Peng, *Eur. J. Med. Chem.*,2011, **46**, 3237.
33 C. Y. Li, X. Y. Zhang, M. Zhao, Y. J. Wang, J. H. Wu, J. W. Liu, M. Q. Zheng and S. Q. Peng, *Eur. J. Med. Chem.* 2011, **46**, 5598.
34 E. M. Briso, J. Guinea-Viniegra, L. Bakiri, Z. Rogon, P. Petzelbauer, R. Eils, R. Wolf, M. Rincón, P. Angel and E. F. Wagner, *Genes & development*, 2013, **27**, 1959.
35 S. J. Koh, J. M. Kim, I. K. Kim, S. H. Ko and J. S. Kim, *Journal of gastroenterology and hepatology*, 2014, **29**, 502.
36 P. M. Rothwell, F. G. R. Fowkes, J .F. Belch, H. Ogawa, C. P. Warlow, and T. W. Meade, *The Lancet*, 2011, **377**, 31.
37 K. Chinen, Y. Tokuda, M. Fujiwara, Y. Fujioka, *Pathology-Research and Practice*, 2010, **206**, 682.
38 Y. Pawitan, L. Yin, A. Setiawan, G. Auer, K. E. Smedby, K. Czene, *European Journal of Cancer*, 2015, **51**, 751.
39 M. Zhao, L. R. Bi, W. Wang, C. Wang, M. Baudy-Floc'h, J. F. Juc, and S. Q. Peng, *Bioorg. Med. Chem. Lett.*, 2006, **14**, 6998.
40 M. Zhao, S. Q. Peng, J. H. Wu, Y. J. Wang and X. Hu, *Patient*, 2013, CN103450338.
41 K. L. Kaestle, M. K.Anwer, T. K. Audhya, and G. Goldstein, *Tetrahedron letters*, 1991, **32**, 327.
42 R. Pignatelloand T. M. G. Pecora, *Die Pharmazie - An International Journal of Pharmaceutical Sciences*, 2007, **62** 663.
43 E. Nawrocka-Bolewska, I. Z. Siemion, M. Mihelić and W. Voelter, *Liebigs Annalen der Chemie*, 1990, **3**, 245.

44 T. Maehama, H. Okura, K. Imai, K. Saito, R. Yamada, T. Koyama, A. Hayashida, Y. Neihi, T. Kawamoto and K. Yoshida, *J. Cardiol.*, 2010, **56**, 118.
45 J. H. Wu, Y. J. Wang, Y. N. Wang, M. Zhao, X. Y. Zhang, L. Gui, S. Y. Zhao, H. M. Zhu, J. H. Zhao and S. Q. Peng, *Int. J. Nanomed.*, 2015, **10**, 2925.
46 S. Li, Y. J. Wang Y, F. Wang, Y. N. Wang, X. Y. Zhang, M. Zhao, Q. Q. Feng, J. H. Wu, S. Y. Zhao, W. Wu and S. Q. Peng, *Int. J. Nanomed.*, 2015, **10**, 5273.

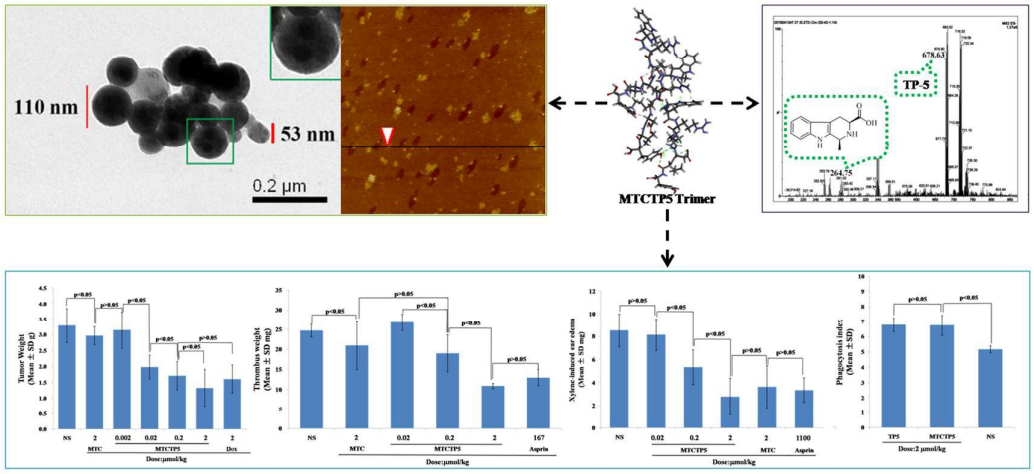

The nano-feature, release, bioactivities and action mechanism of β-carboline-thymopentin conjugate, a novel nanomedicine, were presented.